

Chloroaluminum phthalocyanine thin films: chemical reaction and molecular orientation

Florian Lattayer · Heiko Peisert · Johannes Uihlein ·
Tamara Basova · Peter Nagel · Michael Merz ·
Stefan Schuppler · Thomas Chassé

Received: 13 November 2012 / Revised: 13 February 2013 / Accepted: 14 February 2013 / Published online: 14 March 2013
© Springer-Verlag Berlin Heidelberg 2013

Abstract The chemical transformation of the polar chloroaluminum phthalocyanine, AlClPc, to μ -(oxo)bis(phthalocyaninato)aluminum(III), (PcAl)₂O, in thin films on indium tin oxide is studied and its influence on the molecular orientation is discussed. The studies were conducted using complementary spectroscopic techniques: Raman spectroscopy, X-ray photoelectron spectroscopy, and near-edge X-ray absorption fine structure (NEXAFS) spectroscopy. In addition, density functional theory calculations were performed in order to identify specific vibrations and to monitor the product formation. The thin films of AlClPc were annealed in controlled environmental conditions to obtain (PcAl)₂O. It is shown that the chemical transformation in the thin films can proceed only in the presence of water. The influence of the reaction and the annealing on the molecular orientation was studied with Raman spectroscopy and NEXAFS spectroscopy in total electron yield and partial electron yield modes. The comparison of the results obtained from these techniques allows the determination of the molecular orientation of the film as a function of the probing depth.

Keywords Interface/surface analysis · Thin films · Chloroaluminum phthalocyanine

Introduction

Phthalocyanines (Pcs) are of interest for a variety of optoelectronic devices, the commonest applications being field-effect transistors [1, 2], solar cells [3, 4], and light-emitting diodes [3]. The broad bandwidth for applications of Pcs results from their electronic and optical properties which can be tailored by chemical modifications. Substituents can be introduced at the peripheral positions or at the central atom. Substitution at the periphery, for example, with aliphatic [5, 6] or aromatic [7] moieties, induces, for example, liquid-crystalline properties, whereas substitution with oxygen [8, 9], chlorine [10, 11], or fluorine [12] at the central metal creates a permanent dipole moment. Moreover, sandwich complexes [12–14] and annulated Pcs [15, 16] are known.

Polar Pcs have been investigated intensively recently. In contrast to the more familiar CuPc or ZnPc, the polar metal Pcs are not planar but are umbrella-like and tilted by 7°, leading to a symmetry lowering from D_{4h} to C_{4v} . Nevertheless, the vibrational structure of peripheral unsubstituted Pcs, for example, in Raman spectroscopy, is very similar between D_{4h} and C_{4v} [17, 18].

It can be expected that the presence of a molecular dipole moment offers a route to control the growth of molecules in thin films by means of external factors. Indeed, it was shown for TiOPc [9], AlClPc [10, 19], and VOPc [8] that electric and magnetic fields can influence the molecular orientation, the polymorphism, and the surface morphology. On the other hand, it can be shown that for devices containing Pcs as active layers, the efficiency is affected by the growth, interface properties [20–23], molecular orientation [10, 11,

F. Lattayer · H. Peisert (✉) · J. Uihlein · T. Chassé
Institut für Physikalische und Theoretische Chemie, Universität
Tübingen, Auf der Morgenstelle 18,
72076 Tübingen, Germany
e-mail: heiko.peisert@uni-tuebingen.de

T. Basova
Nikolaev Institute of Inorganic Chemistry,
Russian Academy of Sciences, Lavrentiev Pr., 3,
630090 Novosibirsk, Russia

P. Nagel · M. Merz · S. Schuppler
Institut fuer Festkörperphysik (IFP), Karlsruhe Institute
of Technology (KIT),
76021 Karlsruhe, Germany

21, 24], and electronic properties [25–27]. In this context, possible chemical reactions in air are important.

The reaction from AlClPc to $(\text{PcAl})_2\text{O}$ in solution has been already described in the literature [28, 29]. It was shown that the hydrolysis of AlClPc upon immersion in KCl water solutions at different pH values leads via hydroxyaluminum phthalocyanine, $\text{Al}(\text{OH})\text{Pc}$, finally to the formation of μ -(oxo)bis(phthalocyaninato)aluminum(III), $(\text{PcAl})_2\text{O}$ [28].

In a previous article [19] the influence of a magnetic field (1 T), applied during postdeposition annealing, on AlClPc films was studied. The reaction from AlClPc to $(\text{PcAl})_2\text{O}$ on the substrate surface on annealing in air under ambient conditions was monitored by UV/vis spectroscopy, IR spectroscopy, Raman spectroscopy, X-ray photoelectron spectroscopy (XPS), and atomic force microscopy.

The aim of this work is a more detailed investigation of the chemical reaction from the monomer AlClPc to $(\text{PcAl})_2\text{O}$ μ -(oxo)dimers in thin films deposited on indium tin oxide (ITO). We focus on the study of the influence of environmental conditions as well as the molecular orientation. The reaction from AlClPc to $(\text{PcAl})_2\text{O}$ on the substrate surface in controlled environmental conditions was investigated by Raman spectroscopy and XPS. To assign the vibrations and their corresponding symmetry of the monomer and the μ -(oxo)dimer, density functional theory (DFT) calculations were used for comparison with the experiment findings. The identification of significant bands with their specific symmetry makes possible the investigation of the molecular orientation with Raman spectroscopy in combination with near-edge X-ray absorption fine structure (NEXAFS) spectroscopy.

Experimental

Materials

AlClPc was synthesized as described earlier [19]. The structures of AlClPc and $(\text{PcAl})_2\text{O}$ as ball and stick models and the formal reaction are shown in Fig. 1. Additionally, a skeletal structure of AlClPc is given. The structure and

stoichiometry were checked by XPS and Raman spectroscopy; in particular, the presence of μ -(oxo)dimers in the source material can be ruled out. The film thickness was estimated from XPS intensities assuming layer-like growth. The inelastic mean free path was calculated according to the method described in [30]: we obtained about 2.4 nm for C 1s electrons with a kinetic energy of approximately 966 eV (corresponding to an information depth of about 7 nm). The Al/Cl elemental ratio was determined to be 1:1 from Al 2p and Cl 2p core level spectra using corresponding sensitivity factors from [31]. The Raman fingerprint spectrum of AlClPc was used to identify the structure [10, 11, 17]. Beam damage in XPS and NEXAFS spectroscopy was ruled out by the observation of possible changes of the peak shape of the C 1s spectrum during the measurements. In the case of Raman spectroscopy, during the typical measurement time (approximately 5 min per spectrum), no spectral changes were observed.

The ITO substrate was cut and cleaned ex situ with acetone and ethanol in an ultrasonic bath before film deposition. ITO was used as a substrate because it is used as an electrode material in devices.

Methods and preparation

The thin films of AlClPc with nominal film thicknesses of 50 nm were prepared by physical vapor deposition from a temperature-controlled cell with an evaporation rate of $0.5 \text{ nm} \cdot \text{min}^{-1}$ on ITO substrates in a ultra-high-vacuum preparation chamber with a base pressure of 6×10^{-10} mbar. The films were characterized with XPS directly after deposition. Subsequently Raman and UV/vis spectra were measured under ambient conditions. It was verified by XPS that exposure to air at room temperature does not lead to a chemical reaction. The subsequent annealing at 300 °C for 1–1.5 h initiates the reaction forming the μ -(oxo)dimer. The annealing of the films was performed in different controlled environmental conditions in a separate closed-chamber system as described earlier [32]. The environmental conditions used were (1) dry N_2 (purity 5.0), (2) N_2 saturated with H_2O

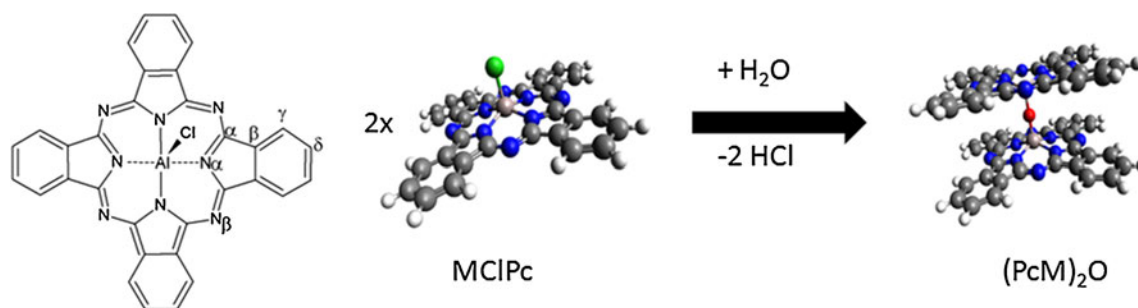


Fig. 1 Left: Structure of chloroaluminum phthalocyanine (AlClPc) with labeled C and N. Right: Formal reaction of the dimerization of MCIPc to $(\text{PcM})_2\text{O}$. Different atoms appear in different colors (hydrogen white, carbon gray, nitrogen blue, aluminum rose, chlorine green, oxygen red)

(N₂/H₂O) (more than 95 % relative humidity), and (3) ambient conditions (exposure to air). Before the annealing, the chamber was purged for 2 h with the corresponding gases to establish a constant environment. The deposited films were characterized by XPS after deposition. The films which were investigated by NEXAFS spectroscopy were prepared in our laboratory and were characterized with XPS, Raman spectroscopy, and UV/vis spectroscopy prior to the NEXAFS measurements.

XPS spectra were measured in a separate chamber using Mg K α radiation and a hemispherical EA 125 analyzer (Omicron); the base pressure was 4×10^{-10} mbar. Pass energies of 50 and 30 eV were used for overview and detailed spectra, respectively. Since no substrate signals were observed for the films with nominal thicknesses of 50 nm, the energies were calibrated to the C 1s peak maximum of AlClPc of 284.6 eV (as found for thin films with a thickness of 2–8 nm).

The Raman measurements of the thin films were performed with a confocal Raman spectrometer (LabRam HR800 equipped with a BX 41 microscope) from Horiba Jobin-Yvon. A long-distance lens with 50-fold magnification and a numerical aperture of 0.5 was used. The spatial resolution (central lobe diameter) for this lens is approximately 1.3 μ m and the estimated field depth is estimated to be 3.2 μ m.

The spectra were recorded in backscattering geometry using a frequency-doubled Nd:YAG laser (30 mW) with an excitation wavelength of 532 nm. The incoming laser light was attenuated by 90 % to reduce the influence of local heating. An edge filter cut the Rayleigh line up to 120 cm⁻¹. A grating with 600 lines per millimeter was used, and the spectral resolution was about 3 cm⁻¹.

NEXAFS spectra were recorded at the ANKA synchrotron radiation source (Karlsruhe, Germany) at the WERA beamline. The energy resolution at the NK edge was set to approximately 200 meV, and the degree of linear polarization was more than 95 %. The NEXAFS spectra were measured in total electron yield (TEY) (sample current) and partial electron yield (PEY) (channeltron) mode. The TEY and PEY spectra were recorded in parallel at the same spot and at the same time. The spectra were normalized to equal step heights. To evaluate the π^* resonances, the areas were estimated by numerical integration of the region from 397.5 to 402 eV (shaded areas in Fig. 6), assuming that the edge structure is at higher photon energies.

DFT calculations of vibrational frequencies were performed using Gaussian 09 at the B3LYP/6-311++G** level of theory to study the geometry and vibrational frequencies. All structures represent minima on the corresponding hypersurface since no imaginary frequencies were found. The wavenumbers obtained from each calculation were scaled by a factor of 0.978. We will not discuss Raman intensities since the intensity of a mode depends on several parameters, for example, the laser wavelength, molecular interactions, and the molecular orientation, which is not taken into account for a single molecule.

Results and discussion

Characterization of the thin films and the reaction

Raman spectroscopy is very sensitive to the molecular and crystal structure as well as to the symmetry of the molecule.

Table 1 Comparison of experimental and calculated frequencies of chloroaluminum phthalocyanine—AlClPc—and μ -(oxo)bis(phthalocyaninato)aluminum (III)—(PcAl)₂O—at the B3LYP/6-311++G(d,p) level of theory and scaled by a factor of 0.978

Experimental (cm ⁻¹)	Calculated (cm ⁻¹)	Symmetry	Assignment
AlClPc			
173	164	A ₁	ν (Al–Cl)
292	286	A ₁	ν (Al–Cl)
352	350	A ₁	ν (Al–Cl)
487	483	E	ν (Al–Cl)
589	588	A ₁	Ring breathing
680	680	A ₁	Ring breathing
829	831	A ₁	Ring breathing
1,538	1,518	E	Central atom specific
(PcAl) ₂ O			
272	261	A _{1g}	ν (Al–O–Al)
304	305	A _{1g}	ν (Al–O–Al)
346	342	E _g	δ (Al–O–Al)
586	588	A _{1g}	Ring breathing
682	679	A _{1g}	Ring breathing
831	831	A _{1g}	Ring breathing
1,533	1,515	E _g	Central atom specific

DFT calculations of wavenumbers are widely used to identify substances, vibrational modes, and their corresponding symmetry. The focus here is on the vibrational modes corresponding to parts of the molecules which change after the reaction, i.e., on the μ -(oxo)dimer (PcAl)₂O. For comparison, we performed calculations for AlClPc, and these were in good agreement with the literature [10].

The DFT calculations predict D_{4h} symmetry for the μ -(oxo)dimer (PcAl)₂O, whereas the monomer AlClPc possesses C_{4v} symmetry. Similar Raman wavenumbers are therefore expected, since the main rotational axis is the same (fourfold). Most of the Raman peaks are related to vibrations of the Pc ring system, and thus the general appearance of the spectrum can be seen as a fingerprint for Pcs [33, 34].

The most relevant vibrational modes are Al–Cl modes which evolve to Al–O–Al modes during the chemical reaction. Table 1 shows the calculated wavenumbers for the monomer and the μ -(oxo)dimer; these are compared with the experimental values and are discussed later. Totally symmetric modes were used for the determination of the molecular orientation. The central metal atom specific mode is also given since a change of the chemical surroundings at the central metal atom is expected.

If the theoretical wavenumbers of the Al–Cl (in AlClPc) and Al–O–Al [in (PcAl)₂O] vibrations are compared, significant changes in the low-wavenumber regions are expected because the modes at 164, 286, and 483 cm⁻¹ (Al–Cl) vanish and new modes at 261 and 305 cm⁻¹ (Al–O–Al) develop (see Table 1). The Al–Cl mode at about 350 cm⁻¹, however, is close to the new expected Al–O–Al mode at 342 cm⁻¹. Very minor changes are expected for the energy positions of those totally symmetric modes—at (1) 588, (2) 680, and (3) 831 cm⁻¹—which represent ring breathing vibrations, and the ring remains essentially unaffected during the reaction. The alteration of the chemical surroundings at the central atom causes a small shift of 3 cm⁻¹ to lower wavenumbers of the central atom specific mode.

Figure 2a–c shows specific parts of experimental Raman spectra of nominal 50-nm AlClPc thin films on ITO as deposited and after annealing in different defined environmental conditions. The Raman spectra have been separated into three different regions to give a more detailed view since the intensities vary strongly across the spectra. We show spectra for a freshly prepared thin film (black lines), a thin film after annealing in a nitrogen environment (red lines), a thin film after annealing in a nitrogen environment saturated with water (blue lines), and a thin film after annealing under ambient conditions (green lines).

Peak positions of the freshly prepared AlClPc thin film can be found quite close to the calculated wavenumbers for AlClPc and demonstrate good agreement between theory and experiment. One of the reasons for the remaining small

differences (see Table 1) can be ascribed to the fact that the DFT calculations were performed for a single molecule and the variations may indicate solid-state effects. The spectrum of the film annealed in a nitrogen environment is very similar to the spectrum of the untreated film, pointing to the absence of a chemical reaction.

The Raman spectra for the films annealed in nitrogen saturated with water (N₂/H₂O) or under ambient conditions appear similar to each other but are different from the spectra for the freshly prepared film and the film annealed in N₂. Similar spectra were recently reported for (PcAl)₂O [19, 35]. We discuss the spectra corresponding to the reaction under ambient conditions exemplarily (see Fig. 2) in detail. From a comparison of the Raman spectra before and after the reaction (black and green lines) only minor changes are visible in Fig. 2b and c. The experimentally found vibrations with considerable contribution from ν (Al–Cl) are located at 173, 292, 352, and 487 cm⁻¹. They exhibit very low intensity compared with other vibrations because of small changes in the polarizability, and therefore they might be partly overlapped by vibrations of the Pc ring system. In Fig. 2a, these Al–Cl bands have nearly vanished in the spectra corresponding to the films after the reaction and new modes close to the wavenumbers of Al–Cl are assigned to Al–O–Al vibrations, in agreement with theory.

The totally symmetric bands representing the Pc ring are observed at 589, 680, and 829 cm⁻¹ in Fig. 2b and their spectral positions do not change significantly after the reaction, as expected from the calculations. Some new modes develop next to the mode at 589 cm⁻¹, indicating new vibrational structures. Another significant change can be observed in the region between 800 and 900 cm⁻¹ [19]. The totally symmetric band at 829 cm⁻¹ can be assigned from DFT calculations to a ring breathing, in agreement with recent calculations [10]. An additional band at 846 cm⁻¹ next to the totally symmetric mode at 830 cm⁻¹ can be found which decreases in intensity after the reaction as seen in the dashed boxes. According to the calculated wavenumbers, there is no single-molecule Raman active vibration at 846 cm⁻¹. Therefore, we presume that the band is related to Davydov splitting, in agreement with findings for other Pcs [10, 11, 36].

The central atom specific mode for AlClPc is found experimentally at slightly higher wavenumbers (1,538 cm⁻¹) compared with theory in Fig. 2c, which could be related to intermolecular interactions between the molecules [33]. The main contribution to this vibration is given by displacements of the C_α–N_β–C_α bridge bonds of the Pc macrocycle. Considering in detail the central metal atom specific mode in the Raman spectra, the energy positions shift to 1,533 cm⁻¹ after the reaction. The shift of 5 cm⁻¹ to lower wavenumbers indicates a change in the central atom surroundings. From DFT, a peak shift of 3 cm⁻¹ to lower wavenumbers is expected

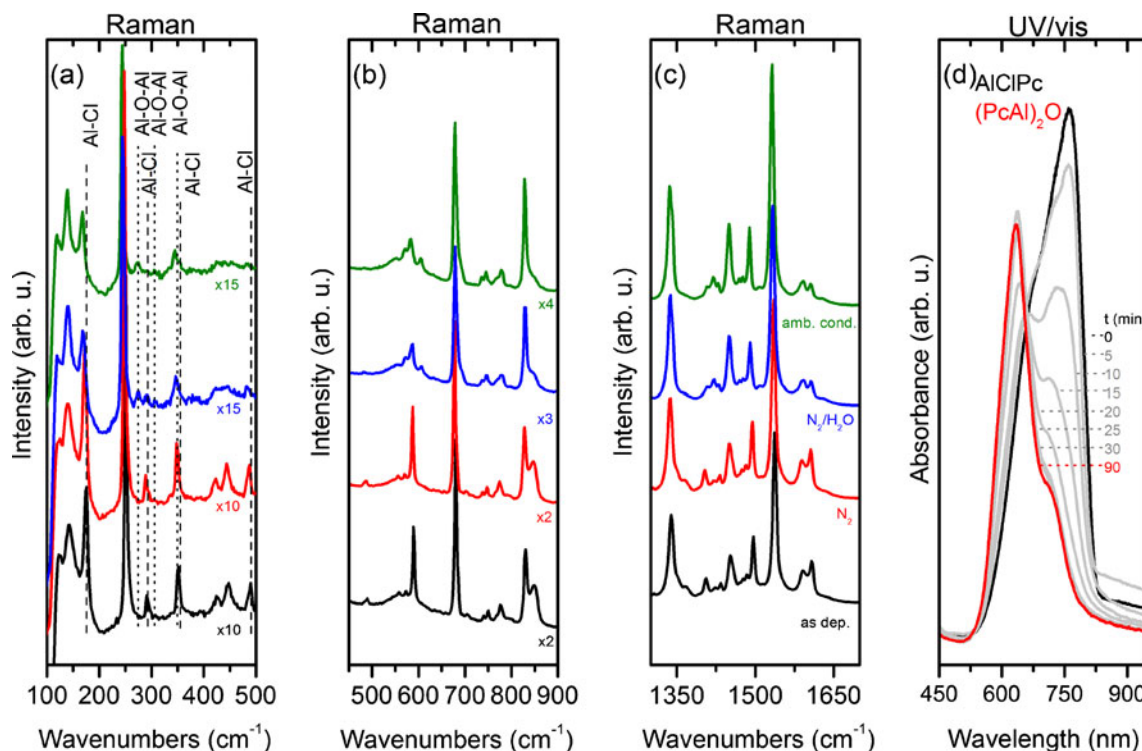


Fig. 2 **a–c** Experimental Raman spectra of 50-nm thin films of AIClPc/indium tin oxide (ITO) annealed in controlled environmental conditions: as deposited (*black lines*), after annealing in nitrogen (*red*

lines), after annealing in nitrogen saturated with water (*blue lines*), and after annealing under ambient conditions (*green lines*). **d** Time-dependent UV/vis spectra of the thin film annealed at 300 °C for 90 min

because of the reaction, which fits well to the experimental observation (see Table 1).

We note that no –OH-related vibration was observed for the annealed AIClPc films with Fourier transform IR spectroscopy (not shown). The nonappearance of an –OH peak, expected between 3,400 and 3,700 cm^{-1} , indicates the absence of formation of Al(OH)Pc and a nearly quantitative transformation of AIClPc to (PcAl)₂O in the films.

The progress of the reaction from AIClPc to (PcAl)₂O was also monitored by time-dependent UV/vis spectroscopy (Fig. 2d). Before annealing (black curve), the maximum is located at 750 nm, indicating a triclinic phase of AIClPc [37]. After the reaction this maximum is only visible as a shoulder shifted by 35 nm to 715 nm. Spectra were taken every 5 min for a total of 30 min (gray lines) to monitor the progress of the reaction in the film. The final spectrum after 90 min drawn in red shows two maxima, at 750 and 630 nm; the shape is in good agreement with the shape of the literature spectra of (PcAl)₂O [35]. Already the spectrum measured after 20 min coincides quite well with the spectrum after 90 min, indicating that the reaction in the film is practically complete at 300 °C under ambient conditions.

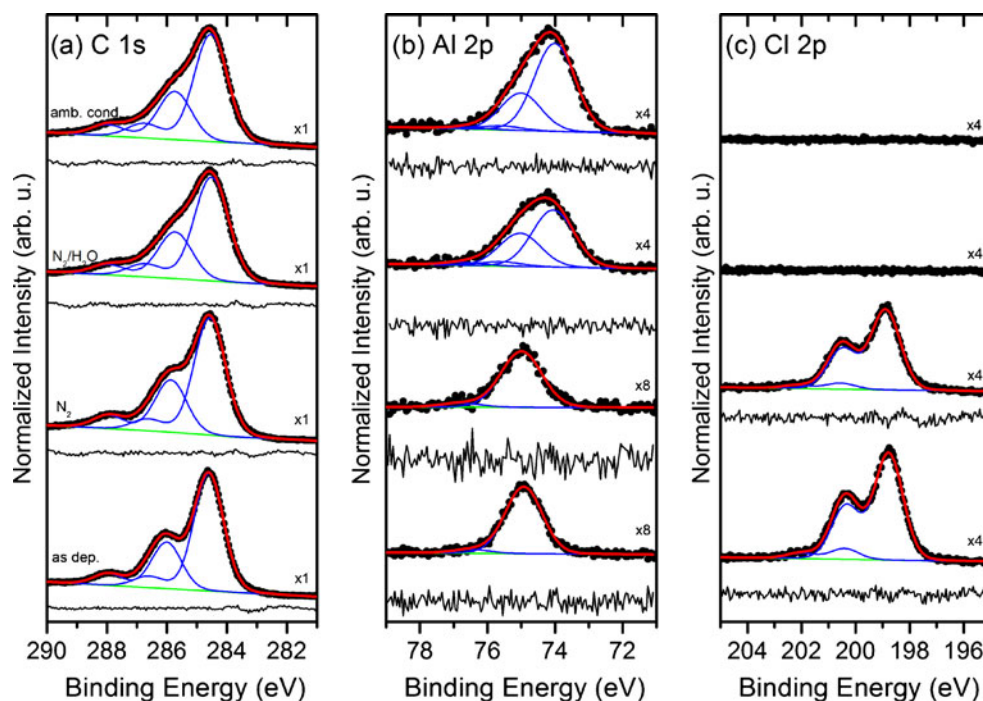
XPS measurements can provide additional and supporting information about the chemical state of particular atoms. The AIClPc films were prepared in an ultrahigh vacuum with nominal film thicknesses of 50 nm and were characterized

by XPS immediately after deposition and after subsequent annealing in different environmental conditions. The corresponding XPS core level spectra for carbon, aluminum, and chlorine are depicted in Fig. 3. The spectra of the as-deposited thin films (at the bottom in Fig. 3) are compared with the spectra obtained after annealing in N₂, in N₂ plus water, and in ambient conditions. The intensities of the particular core level have been normalized to the maximum of the corresponding C 1s spectrum. We note that no oxygen signal is observed after preparation.

The C 1s core level spectra were fitted with four Voigt functions [38, 39]. An intensity ratio of 3:1 was assumed for the peak fitting related to the atomic ratio (C–H, C–C):(C–N). The C 1s spectrum of the freshly prepared film exhibits a C–C/C–H signal at 284.6 eV and a C–N signal at 286.0 eV. The two additional peaks at higher binding energies of 286.6 and 287.9 eV are assigned to shake-up satellites [39–41]. The binding energies of C 1s and N 1s core level spectra are in good agreement with those for other metal Pcs [20, 42]. For a more detailed discussion of the C 1s peak shape, see [38, 42]. The Cl 2p and Al 2p spectra of the as-deposited AIClPc film can be described essentially by one doublet; the binding energies of the 2p_{3/2} component are 198.8 and 75.0 eV, respectively. The values are in good agreement with the literature values [19].

After the annealing of the AIClPc films in a dry nitrogen environment (red curves in Fig. 3), no significant changes

Fig. 3 Peak-fitted core level spectra of AICIPc thin films on ITO annealed in different controlled environmental conditions: as deposited, annealed in an N_2 environment, annealed in an N_2 environment saturated with water, and annealed under ambient conditions. The intensities of the particular core level have been normalized to the maximum of the corresponding C 1s spectrum. The fits, with the residuals below each fit, are described in the text



were observed in the particular core level spectra; all the spectra were fitted using the same shape. Only a slight broadening of the C 1s spectra was found (the full width at half maximum of the Gaussian increases from 1.11 to 1.18 eV), which might be attributed to a change of the morphology of the film. This is in good agreement with the results obtained by Raman spectroscopy, where also no changes were observed after annealing in an N_2 environment (see earlier).

In contrast, annealing in the presence of water leads to significant spectral changes in the core level spectra. The Cl 2p signal in Fig. 3c disappears, which indicates that the Cl is completely removed at least for the related XPS probing depth of about 7 nm. A further hint at a change in the chemical bonding of the metal atom is an energy shift of the corresponding Al 2p core level spectra towards lower binding energies by about 0.7 eV. Such chemical shifts to lower binding energies in XPS point to a higher electron density at the central atom, which might be expected for $(PcAl)_2O$ (since oxygen is neighbored by two Al atoms). Even though the description with a single doublet does not result in optimal peak fitting results (see the residuals), from Raman data we rule out the presence of other oxidation products such as Al–OH. Rather we ascribe the inhomogeneous broadening to a nonuniform environment (see later).

On the other hand, the shape of the C 1s peak does not change drastically on the reaction in N_2/H_2O , and the binding energy of C–H is still at 284.6 eV. The C–N peak is shifted slightly to lower binding energies (200 meV), which might be related to higher electron densities due to the new chemical environment around the central atom. The absence of new peaks in the C 1s (and N 1s) spectra indicates that the Pc ring

is not significantly altered in the course of the reaction. The distinct broadening of the core level spectra might be due to a nonuniform environment of the Pc macrocycles after the reaction and/or the inhomogeneous adsorption of water. Since the reaction proceeds in an N_2/H_2O environment excluding oxygen, we conclude from Raman and XPS data that for the reaction from the polar AICIPc to the μ -(oxo)dimer only water is needed, and oxygen from air does not seem to be essential for the chemical reaction.

Influence of the reaction on the molecular orientation

The question now arises whether the chemical reaction affects the molecular orientation in the film significantly. Raman spectroscopy and NEXAFS spectroscopy have been successfully applied recently to investigate the molecular orientation in thin films even on relatively ill defined ITO substrates [11, 20, 43]. We note that the different information depth and Raman and NEXAFS spectroscopy were recently also used for related systems such as perylene-3,4,9,10-tetracarboxylic-3,4,9,10-dianhydride (PTCDA) and N,N'-dimethyl-3,4,9,10-perylene tetracarboxylic diimide (DiMe-PTCDI) on GaAs (100) [44]. Another example of the combined use of optical spectroscopies (IR reflection–absorption spectroscopy) and NEXAFS is in the investigation of the orientation of self-assembled monolayers on Au (111) [45].

First, we will discuss polarized Raman spectra taken in parallel $z(xx)\bar{z}$ and cross $z(xy)\bar{z}$ polarization in Fig. 4 (notation corresponding to that in [46]). To describe the molecular orientation, we use Euler coordinates [11, 43,

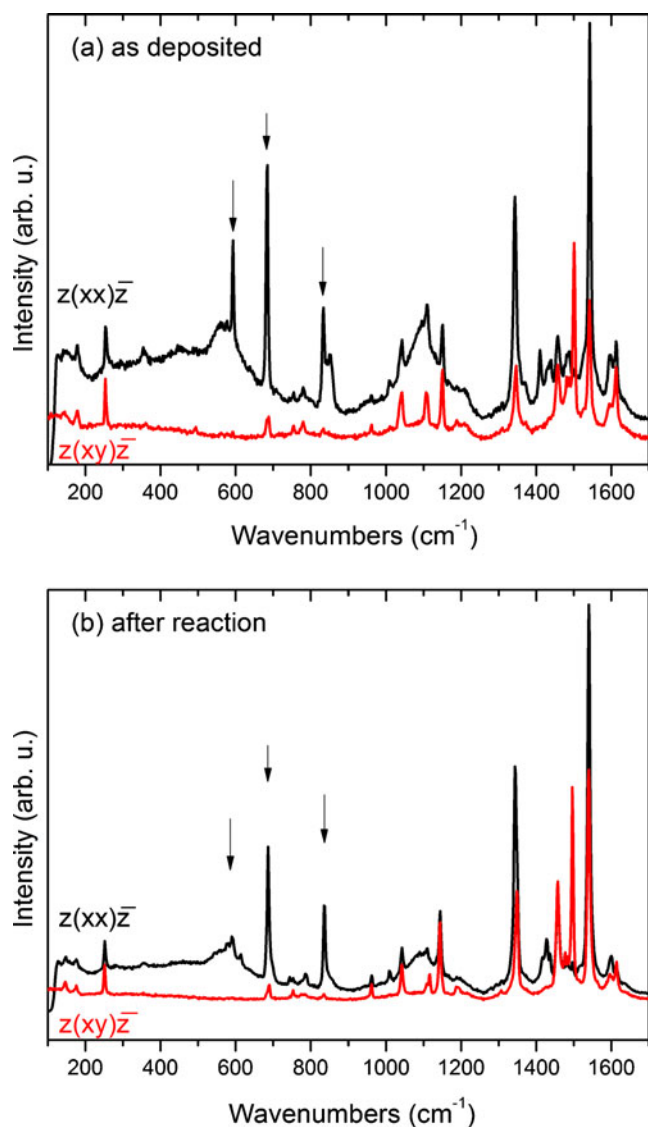


Fig. 4 Example of polarized Raman spectra of an AlClPc film before annealing (a) and after the reaction (b). The totally symmetric A_1/A_{1g} modes which are used for the orientation analysis are marked with arrows

47, 48] but Cartesian coordinates [7, 9, 10, 49] can also be successfully applied. If an azimuthally averaged orientation model is assumed in an Euler coordination system, totally symmetric modes (see Table 1) are uniquely sensitive to the tilt angle ϑ of the molecule relative to the substrate surface [11]. This angle is additionally comparable to the tilt angles obtained with NEXAFS spectroscopy discussed below.

The basic approach for the determination of the molecular orientation by Raman spectroscopy is known from the literature [11, 43]. Since no azimuthal anisotropy of the depolarization ratio ρ was observed, we applied the model for an azimuthally averaged molecular orientation [11]. The transformation from molecular to substrate coordinates is

performed followed by the azimuthal averaging around the angle φ according to

$$I_{\parallel/\perp} = \int_0^{2\pi} \left(e_i^{\parallel} \cdot \left(R(\phi, \vartheta, \psi)^T \cdot A_{1g}^{\parallel/\perp} \cdot R(\phi, \vartheta, \psi) \right) \cdot e_s^{\parallel/\perp} \right)^2 d\phi.$$

The ratio between intensities measured using cross-polarized and parallel-polarized light is defined as the depolarization ratio ρ and can be calculated from parallel-polarized and cross-polarized Raman spectra [11, 43, 49]. The inclination angle of the molecule, i.e., the Euler angle ϑ , is obtained by comparison of the experimental depolarization ratio with calculated values.

Figure 4a shows the polarized Raman spectra directly after deposition of the AlClPc film, whereas the typical spectra in Fig. 4b correspond to a film after the reaction. The evaluated totally symmetric A_1 (Fig. 4a) and A_{1g} (Fig. 4b) modes are marked with arrows. Initially, before annealing, the depolarization ratio is about 0.08. This corresponds to an Euler angle ϑ of 52° , which is close to the magic angle. This depolarization ratio points to less ordered structures or strongly inclined molecules in the bulk as recently discussed [11]. The depolarization ratio after the reaction is about 0.07, corresponding to an Euler angle ϑ of 50° —similar to the initial value, indicating a less ordered film. The values are related to the bulk of the film since signals of the ITO background are found before and after the reaction in the regions between 500 and 700 cm^{-1} and 900 and 1,300 cm^{-1} . The Raman data therefore indicate that the averaged molecular orientation in the AlClPc and (PcAl) $_2$ O thin film obtained by annealing of the as-deposited film is not significantly changed because of the reaction.

However, the orientation may change as function of the film thickness or may be different at the interface or surface [20]. Therefore, the surface-sensitive NEXAFS spectroscopy method was applied to investigate this question in more detail. The surface sensitivity of NEXAFS spectroscopy depends further on the detection mode used. In the case of TEY mode, all electrons that emerge from the surface are (indirectly) detected, and slow secondary electrons of about 5 eV dominate the signal. Since these electrons can escape from the sample after several inelastic scattering processes, they originate to a large extent from layers deeper than the mean free path of the electrons. On the other hand, for PEY detection, the retarding voltage of the detector determines the kinetic energy of the electrons (in our case higher than 350 eV), and essentially specific Auger electrons are detected. This results in a sampling depth of about 1–2 nm for PEY NEXAFS spectroscopy and about 10 nm for TEY NEXAFS spectroscopy [50]. The different information depth of all methods is illustrated in Fig. 5: Whereas the

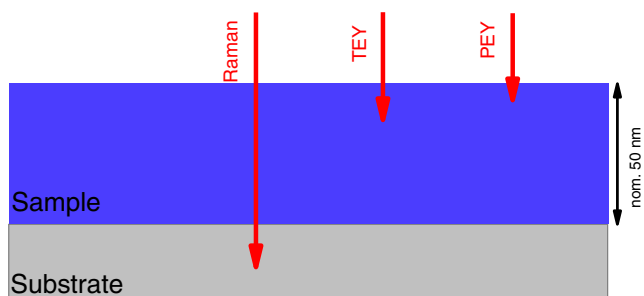


Fig. 5 The probing depth for the different measurements: Raman, total electron yield (TEY), partial electron yield (PEY)

laser beam in Raman spectroscopy penetrates through the whole film, TEY and PEY in NEXAFS spectroscopy are sensitive to the uppermost layers (see earlier).

For Pcs, the molecular orientation can be probed by monitoring the relative intensities of N $1s \rightarrow \pi^*$ excitations [20]. The spectral features at photon energies below 402 eV correspond essentially to N $1s \rightarrow \pi^*$ transitions and at photon energies above 402 eV they are described mainly by N $1s \rightarrow \sigma^*$ transitions [11, 20]. For a more detailed characterization of the resonances, we refer to the literature [51, 52].

N K-edge absorption spectra were taken from AICIPc films before and after the reaction in TEY mode and PEY mode. Selected spectra are displayed in Fig. 6 as a function of the incidence angle of the p-polarized synchrotron radiation for $\theta=10^\circ$ (grazing incidence) and $\theta=90^\circ$ (normal incidence). Changes of the linear dichroism are more clearly visible in the corresponding difference spectra ($90^\circ - 10^\circ$). The spectra of the as-deposited film show a similar tendency for both modes (TEY, PEY): the maxima of the N $1s \rightarrow \pi^*$ excitations are observed at grazing incidence ($\theta=10^\circ$) in Fig. 6a, pointing to a preferential orientation of the molecular plane perpendicular to the substrate surface (preferred lying absorption geometry). After the reaction, the dichroism appears weaker (Fig. 6b) in particular for spectra taken in TEY mode.

Comparing the relative intensities at 90° and 10° generally allows the estimation of the molecular tilt angle under the assumption of a uniform molecular tilt in the probed sample area and depth; we obtained about $40\text{--}45^\circ$ with respect to the substrate surface. We note, however, that even small systematic errors (inhomogeneous sample, contributions of differently polarized transitions, background correction and

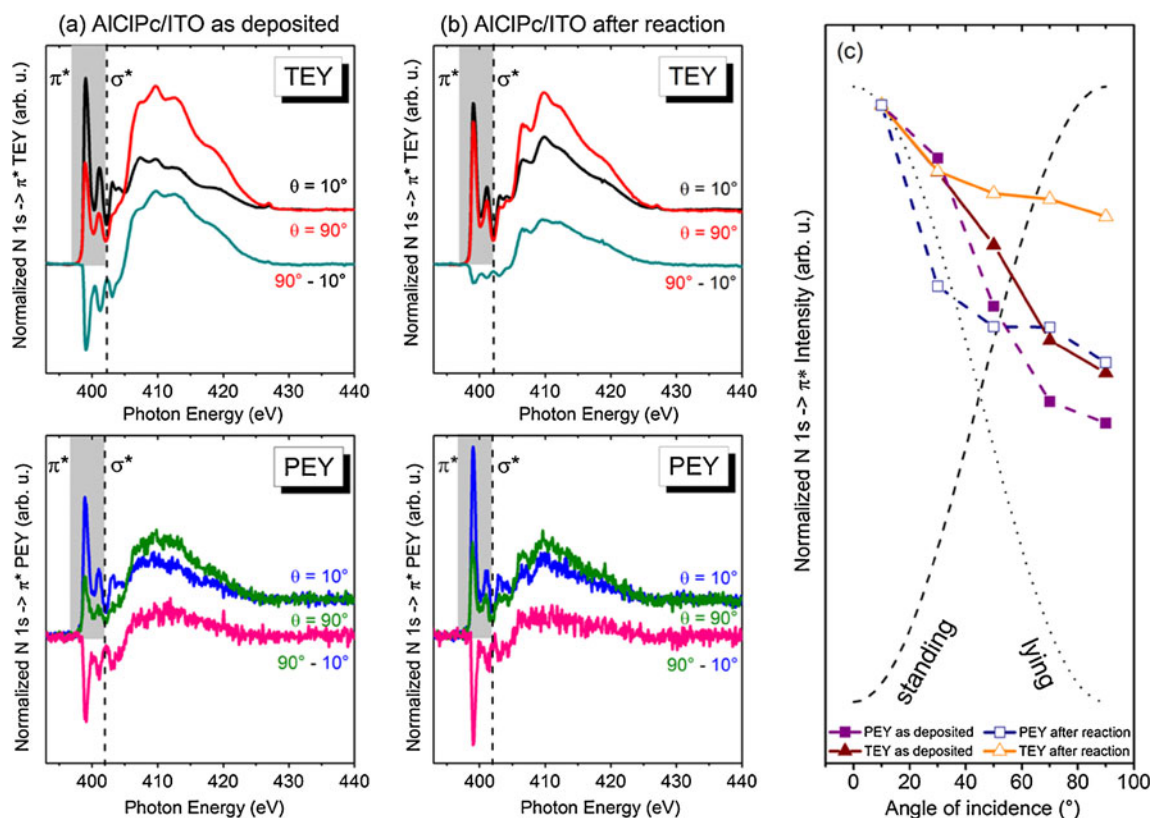


Fig. 6 a, b Near-edge X-ray absorption fine structure spectra with included difference spectra of AICIPc for the as-deposited film (a) and after annealing (b). The upper panels show spectra measured in TEY mode, and the lower panels show spectra measured in PEY mode. The angles given denote the incidence angle of the incoming p-polarized light relative to the substrate. c Angular dependence of the intensity of

the π^* resonances for the as-deposited film and the annealed film. The expected intensity profiles for lying and standing molecules are indicated by the dotted line and the dashed line, respectively. The different behavior of the intensities from spectra measured in TEY and PEY modes points to a different orientation of the uppermost layer with respect to the bulk

normalization, unknown position and width of the step edge, etc.) result in uncertainties, which are in particular large for small molecular tilt angles, as discussed in [20]. The angular dependence of the N 1s- π^* resonance intensity is summarized quantitatively for all measured angles in Fig 6c. The expected functional behavior for perfectly lying and standing molecules assuming a polarization degree of 100 % is plotted as broken lines in Fig. 6c. A tendency for lying molecules is observed for the film before and after the deposition since the angular dependence follows the dotted line for lying molecules, indicating that there is a preferential orientation within the upper 10 nm of the film (with a lower degree of ordering). It is clearly seen that the TEY and PEY intensities show a similar behavior for the as-deposited film.

In contrast, after the reaction, the angular dependencies of the TEY and PEY resonances show a different evolution; the angular dependence of the TEY resonances (more sensitive to the bulk) is less pronounced and indicates less ordered structures similar to the observation using Raman spectroscopy. The angular dependence of the PEY resonances on the other hand (sensitive for the layers close to the surface) is nearly similar to the as deposited film. The differences in the dependence of the molecular orientations on the film thickness might be related to the reorganizational ability of the Pc molecules. Because of the high temperature (300 °C), the molecules may have enough energy to rearrange themselves during the reaction. Because of greater steric hindrance, the molecules in the bulk appear to be less able to rearrange themselves during the reaction, whereas molecules at the surface arrange themselves in a favored geometry comparable to the situation before the reaction. Thus, the molecular orientation seems to be maintained especially close to the surface even after a chemical reaction.

Conclusions

In summary, we investigated the behavior of the dimerization of the polar AICIPc to (PcAl)₂O in thin films on ITO using XPS and Raman spectroscopy. From the annealing in controlled environmental conditions, we conclude that the reaction from AICIPc to (PcAl)₂O occurs in a water environment. Since the presence of oxygen was avoided at temperatures where the oxidation occurs, our data indicate that oxygen from air is not essential for the reaction. The comparative analysis of the theoretical Raman spectra with experimental ones allows clear identification of bands sensitive to the reaction.

The different information depth of PEY, TEY, and Raman spectroscopy offers a route to distinguish between the molecular orientation at the surface and in the bulk. Generally, a low degree of ordering of AICIPc in thin films on ITO is

found in the bulk, whereas close to the surface NEXAFS data show a tendency for lying molecules. The orientation of the uppermost molecules can be partly maintained during the reaction from AICIPc to (PcAl)₂O; most likely the molecules may “rearrange” themselves after the chemical transformation.

For a possible application of AICIPc in devices, it would be very important to protect the materials from water in combination with high temperatures. On the other hand, ultrathin films of oriented (PcAl)₂O might be prepared on substrate surfaces by a reaction of annealed AICIPc in a humid environment.

Acknowledgments We thank W. Neu for technical assistance and V. Kiselev for fruitful discussions. We gratefully thank the bwGRiD project for computational resources. We also acknowledge the ANKA Angstromquelle Karlsruhe for the provision of beam time at the WERA beamline. Financial support from the German Research Council (PE 546/5-1 and CH 132/23-1) is gratefully acknowledged.

References

- Horowitz G (1998) *Adv Mater* 10(5):365–377
- Horowitz G, Hajlaoui ME (2000) *Adv Mater* 12(14):1046–1050
- Armstrong NR, Wang WN, Alloway DM, Placencia D, Ratcliff E, Brumbach M (2009) *Macromol Rapid Commun* 30(9–10):717–731
- Kim DY, So F, Gao YL (2009) *Sol Energy Mater Sol Cells* 93(9):1688–1691
- Dong SQ, Tian HK, Song D, Yang ZH, Yan DH, Geng YH, Wang FS (2009) *Chem Commun* 3086–3088
- Sergeyev S, Pisula W, Geerts YH (2007) *Chem Soc Rev* 36(12):1902–1929
- Basova T, Latteyer F, Atilla D, Gurek AG, Hassan A, Ahsen V, Peisert H, Chassé T (2010) *Thin Solid Films* 518(20):5745–5752
- Kolotovska V, Friedrich M, Zahn DRT, Salvan G (2006) *J Cryst Growth* 291(1):166–174
- Schuster BE, Basova TV, Peisert H, Chassé T (2009) *Chemphyschem* 10(11):1874–1881
- Basova TV, Kiselev VG, Plyashkevich VA, Cheblakov PB, Latteyer F, Peisert H, Chassé T (2011) *Chem Phys* 380(1–3):40–47
- Latteyer F, Peisert H, Aygül U, Biswas I, Petraki F, Basova T, Vollmer A, Chassé T (2011) *J Phys Chem C* 115(23):11657–11665
- Wynne KJ (1985) *Inorg Chem* 24(9):1339–1343
- Atilla D, Kilinc N, Yuksel F, Gurek AG, Ozturk ZZ, Ahsen V (2009) *Synth Met* 159(1–2):13–21
- Miyajima K, Okada E, Nakajima A, Kaya K (2003) *Chem Lett* 32(3):280–281
- Zhou F, Zeile U, Hees M, Plies E, Hanack M (1997) *Eur J Cell Biol* 74:83–83
- Dottinger SE, Hohloch M, Hohnholz D, Segura JL, Steinhuber E, Hanack M (1997) *Synth Met* 84(1–3):267–268
- Aroca R, Jennings C, Loutfy RO, Hor AM (1987) *Spectrochim Acta A* 43(6):725–730
- Aroca R, Zeng ZQ, Mink J (1990) *J Phys Chem Solids* 51(2):135–139
- Basova T, Plyashkevich V, Petraki F, Peisert H, Chassé T (2011) *J Chem Phys* 134(12):124703–124708
- Peisert H, Biswas I, Knupfer M, Chassé T (2009) *Phys Status Solidi B* 246(7):1529–1545

21. Huang YL, Wang R, Niu TC, Kera S, Ueno N, Pflaum J, Wee ATS, Chen W (2010) *Chem Commun* 46(47):9040–9042
22. Dick S, Peisert H, Dini D, Hanack M, Cook MJ, Chambrier I, Chasse T (2005) *J Appl Phys* 97(7):073715–073718
23. Kolacyak D, Peisert H, Chassé T (2009) *Appl Phys A Mater* 95(1):173–178
24. Basova TV, Kiselev VG, Schuster BE, Peisert H, Chassé T (2009) *J Raman Spectrosc* 40(12):2080–2087
25. Aristov VY, Molodtsova OV, Maslyuk VV, Vyalikh DV, Zhilin VM, Ossipyan YA, Bredow T, Mertig I, Knupfer M (2008) *J Chem Phys* 128(3):034703–034706
26. Figgis BN, Kucharski ES, Reynolds PA (1989) *J Am Chem Soc* 111(5):1683–1692
27. Keil C, Schlettwein D (2011) *Org Electron* 12(8):1376–1382
28. Santerre F, Cote R, Lalande G, Gastonguay L, Guay D, Dodelet JP (1995) *J Phys Chem* 99(47):17198–17206
29. Santerre F, Cote R, Veilleux G, SaintJacques RG, Dodelet JP (1996) *J Phys Chem* 100(18):7632–7645
30. Seah MP, Dench WA (1979) *Surf Interface Anal* 1(1):2–11. doi:10.1002/sia.740010103
31. Yeh JJ, Lindau I (1985) *At Data Nucl Data Tables* 32(1):1–155
32. Hintz H, Egelhaaf HJ, Peisert H, Chassé T (2010) *Polym Degrad Stab* 95(5):818–825
33. Tackley DR, Dent G, Smith WE (2001) *Phys Chem Chem Phys* 3(8):1419–1426
34. Tackley DR, Dent G, Smith WE (2000) *Phys Chem Chem Phys* 2(18):3949–3955
35. Zeng ZQ, Aroca R, Hor AM, Loutfy RO (1989) *J Raman Spectrosc* 20(7):467–471
36. Saini GSS, Singh S, Kaur S, Kumar R, Sathe V, Tripathi SK (2009) *J Phys-Condens Mater* 21(22):225006–225009
37. Kato K, Saito Y, Ohdaira Y, Shinbo K, Kaneko F (2006) *Thin Solid Films* 499(1–2):174–178
38. Biswas I, Peisert H, Nagel M, Casu MB, Schuppler S, Nagel P, Pellegrin E, Chassé T (2007) *J Chem Phys* 126(17):174704–174705
39. Ottaviano L, DiNardo S, Lozzi L, Passacantando M, Picozzi P, Santucci S (1997) *Surf Sci* 373(2–3):318–332
40. Brena B, Luo Y, Nyberg M, Carniato S, Nilson K, Alfredsson Y, Ahlund J, Martensson N, Siegbahn H, Puglia C (2004) *Phys Rev B* 70(19):195214–195216
41. Peisert H, Knupfer M, Fink J (2002) *Surf Sci* 515(2–3):491–498
42. Zhang L, Peisert H, Biswas I, Knupfer M, Batchelor D, Chassé T (2005) *Surf Sci* 596(1–3):98–107
43. Zahn DRT, Gavrilina GN, Salvan G (2007) *Chem Rev* 107(4):1161–1232
44. Kampen TU, Salvan G, Paraian A, Himcinschi C, Kobitski AY, Friedrich M, Zahn DRT (2003) *Appl Surf Sci* 212:501–507
45. Liu JX, Schupbach B, Bashir A, Shekhah O, Nefedov A, Kind M, Terfort A, Wöll C (2010) *Phys Chem Chem Phys* 12(17):4459–4472
46. Damen TC, Porto SPS, Tell B (1966) *Phys Rev* 142(2):570–574
47. Munisso MC, Zhu WL, Pezzotti G (2009) *Phys Status Solidi B* 246(8):1893–1900
48. Presser V, Schuster BE, Casu MB, Heinemeyer U, Schreiber F, Nickel KG, Chassé T (2009) *J Raman Spectrosc* 40(12):2015–2022
49. Basova TV, Kolesov BA (1998) *Thin Solid Films* 325(1–2):140–144
50. Harris M, Appel G, Ade H (2003) *Macromolecules* 36(9):3307–3314
51. Floreano L, Cossaro A, Gotter R, Verdini A, Bavdek G, Evangelista F, Ruocco A, Morgante A, Cvetko D (2008) *J Phys Chem C* 112(29):10794–10802
52. Holland BN, Peltekis N, Farrelly T, Wilks RG, Gavrilina G, Zahn DRT, McGuinness C, McGovern IT (2009) *Phys Status Solidi B* 246(7):1546–1551